Progress In Electromagnetics Research B, Vol. 20, 19–32, 2010

SPARSE FREQUENCY WAVEFORM DESIGN FOR MIMO RADAR

G. H. Wang and Y. L. Lu

School of Electrical and Electronic Engineering
Nanyang Technological University
Singapore

Abstract—Multiple-input multiple-output (MIMO) radar has superior performance to conventional one. It has been introduced to almost every application field of conventional radar in recent years. In practical application, MIMO radar also faces the problem of congested spectrum assignment, which makes it not possible to have a continuous clear band with large bandwidth. Sparse frequency waveform that contains several individual clear bands is a desirable solution to this problem. In this paper, we propose a method to design sparse frequency waveform set with low sidelobes in autocorrelations and cross-correlations by optimizing an objective function constructed based on Power Spectrum Density requirement and sidelobe performances of waveform set. Thus, besides the property of approximate orthogonality, the designed waveforms obtain the ability of avoiding spectrum interference to/from other users. The waveform is phase-coded and thereby has constant modulus. The effectiveness of the proposed method is illustrated by numerical studies. Practical implementation issues such as quantization effect and Doppler effect are also discussed.

1. INTRODUCTION

Multiple-input multiple-output (MIMO) radar is a new radar concept enjoying extensive studies nowadays [1–7]. In many studies, MIMO radar is supposed to transmit multiple independent waveforms on transmit end so that receivers can separate them and thereby achieve more degrees of freedom in signal processing. In this kind of MIMO radar, waveforms are required to have good sidelobe performance in

Corresponding author: G. H. Wang (wang0330@ntu.edu.sg).

both autocorrelation functions (ACFs) and cross-correlation functions (CCFs). Orthogonal waveform design is therefore an important topic in MIMO radar study. There are many works on this topic [8–11 and papers therein]. The main idea in these papers is to reduce the sidelobe levels in both the ACFs and CCFs by various optimization methods.

In radar and communication applications, a section of clear and continuous wide band has never been available due to the ever increasing spectrum assignment. As MIMO radar has been proposed for many conventional radar applications, it would also face this problem, especially in applications associated with UHF and HF bands [12–15]. Sparse frequency waveform that contains several individual clear bands is a desirable solution to this problem. With sparse frequency waveform, radar systems can avoid spectrum interference from and/or to other customers. Meanwhile, combining several clear bands together can also improve the range resolution as the total bandwidth is increased. However, it could lead to the problem of high range sidelobes. There are many papers that focus on designing sparse frequency waveforms. Most of the works were reviewed in [15]. In [15], sparse frequency transmitting-receiving waveform design was introduced. The main idea is to design the sparse frequency transmitting waveform without sidelobe consideration first and then design the receiving waveform with sidelobe constraint. The main problem of this method is the mismatch caused in the receiver design. Papers [16, 17] then proposed improved method to design sparse frequency transmitting waveform with sidelobe constraint.

When it comes to the problem of designing orthogonal sparse frequency waveforms, there is few work in current literature. In this paper, we extend our works on designing sparse frequency transmitting waveform to MIMO radar. The designed waveforms can simultaneously satisfy the requirements of desired sparse frequency property and low sidelobe levels in both the autocorrelation functions and cross-correlation functions. To achieve this objective, we construct an objective function based on the power spectral density (PSD) requirement and correlation requirement. Then, this objective function is minimized so that the energy in all stopbands is minimized while keeping the sidelobes in ACFs and CCFs as low as possible. This optimization problem is highly nonlinear, and the global minimum is difficult to be achieved through conventional computation method as the one introduced in [15]. In this paper, we employ Particle Swarm Optimization (PSO) algorithm as the optimization engine to obtain an optimal solution to this problem. The waveforms designed by this paper are phase-controlled with constant modulus [18]. Several design examples show the performance of the proposed method along

with discussions on the properties of designed waveforms. Some implementation issues such as Doppler tolerance and quantization effect are also discussed.

This paper is organized as follows. Section 1 gives an introduction. Section 2 presents the methodology for this paper, including the optimization model and a brief introduction to the implementation of PSO algorithm. Section 3 shows some case studies along with discussions. Section 4 makes the conclusion.

2. OPTIMIZATION MODEL AND PSO ALGORITHM

In this section, we will first introduce the waveform model, based on which we then derive the optimization model. Finally, the optimization engine for this problem is briefly introduced.

2.1. Waveform Model and Objective Function

The waveforms designed in this paper are phase-only complex waveforms. The advantage of this kind of waveform is that the waveform modulus is constant over all time duration, so that the transmitter can work under full power condition. We assume that there are N (set size) waveforms to be designed. Each is represented by a sequence of M (sequence length) samples. The n-th waveform is represented by $\mathbf{x}_n = \left[e^{j\phi_{n,1}}, e^{j\phi_{n,2}}, \ldots, e^{j\phi_{n,M}}\right]^T \in C^{M\times 1}$, where $n = 1, \ldots, N$, the superscript T denotes the vector transpose, and $\phi_{n,m}$, $m = 1, \ldots, M$ are unknown phases to be determined. The waveform set, i.e., waveform matrix, is expressed by assembling all N waveforms as

$$\mathbf{X}(\mathbf{\Phi}) = \left[\ \mathbf{x}_1 \quad \ldots \quad \mathbf{x}_N\ \right]_{M\times N} \tag{1}$$

where Φ is the phase vector defined by:

$$\mathbf{\Phi}_{NM\times 1} = [\phi_{1,1}, \phi_{1,2}, \ldots, \phi_{n,m}, \ldots, \phi_{N,M}]^T,\ \ 1 \le n \le N,\ \ 1 \le m \le M. \tag{2}$$

Though we design phase-only waveforms with constant magnitude in this paper, we can easily generalize it to the phase-amplitude joint design method in order to take advantage of more degrees of freedom by introducing varying amplitude for each waveform.

For MIMO radar waveform design, we concern about not only the sidelobe levels in ACFs but also those in CCFs. That is the main difference compared with single waveform design. The mathematical expressions of them are given below.

Firstly, for phase-only digital waveforms, the autocorrelations and crosscorrelations in discrete forms are defined by [8]:

$$ACF(\mathbf{x}_n, k) = \frac{1}{M} \sum_{m=0}^{M-1-|k|} \mathbf{x}_n(m)\mathbf{x}_n^*(m+k), \quad -M < k < M \qquad n = 1, 2, \ldots, N \tag{3}$$

and

$$CCF\left(\mathbf{x}_p, \mathbf{x}_q, k\right) = \frac{1}{M} \sum_{m=0}^{M-1-|k|} \mathbf{x}_p\left(m\right)\mathbf{x}_q^*\left(m+k\right), \quad -M < k < M \qquad p \neq q, p, q = 1, 2, \ldots, N \tag{4}$$

where $ACF\left(\mathbf{x}_n, k\right)$ and $CCF\left(\mathbf{x}_p, \mathbf{x}_q, k\right)$ are the aperiodic autocorrelation function of digital sequence $\mathbf{x}_n$ and the crosscorrelation function of digital sequences $\mathbf{x}_p$ and $\mathbf{x}_q$, respectively. The asterisk denotes the complex conjugate, and k is the discrete time index.

2.2. Objective Functions

As mentioned in the introduction, there are two requirements to meet. One is the PSD requirement, and the other is the correlation requirement. We have two sub-objective functions, named as Obj_{PSD} and Obj_{CF}, representing these two requirements respectively. The total objective function constructed based on these two sub-objective functions can be expressed as:

$$Obj_{Total} = \lambda Obj_{PSD} + (1 - \lambda) \cdot Obj_{CF} \tag{5}$$

where λ, $0 < \lambda < 1$, is a weighting coefficient to balance these two sub-objective functions.

2.2.1. Objective Function for PSD

On each transmitting site, the band assignment is assumed to be available from prior information or from real-time observation. Normally, for monostatic MIMO radar that has its transmitters and receivers collocated, stopband assignment for each transmitter may be the same. But for multistatic MIMO radar that has transmitters and receivers widely distributed, stopband assignment for each transmitter may be different. For the purpose of simplification, we assume the stopband assignment for each waveform to be the same in this paper. Further extension can be easily made. Then, based on the knowledge of band assignment for each waveform, an desired power spectrum distribution in the whole frequency region of interest, say, $[f_1, f_2]$,

where a number of stopbands are distributed, can be set as $P(f)$. For the n-th transmitting waveform, its true PSD is computed through $|x_n(f)|^2$, $n = 1, \ldots, N$, where $x_n(f)$ is the Discrete Fourier Transform of the waveform. The PSD sub-objective function can be written in the form of minimum mean square error (MMSE), i.e., the difference between the desired PSD and true PSD, as

$$\begin{aligned} Obj_{PSD} &= \sum_{n=1}^{N} \int_{f1}^{f2} w_n(f) \left(|x_n(f)|^2 - P(f) \right)^2 df \\ &= \sum_{n=1}^{N} \sum_{r=1}^{N_s} \int_{f_r^1}^{f_r^2} w_n(f) \left(|x_n(f)|^2 - P(f) \right)^2 df \\ &\quad + \sum_{n=1}^{N} \sum_{g=1}^{N_p} \int_{f_g^1}^{f_g^2} w_n(f) \left(|x_n(f)|^2 - P(f) \right)^2 df \end{aligned} \tag{6}$$

where $w_n(f)$ is the weight for frequency f in the n-th waveform. N_s is the number of stopbands, and N_p is the number of passbands. f_r^1 and f_r^2 are the starting and ending points for the r-th stopband. f_g^1 and f_g^2 are the starting and ending points for the g-th passband. Because $\{x_n(f) | n = 1, \ldots, N\}$ are from Discrete Fourier Transform of the waveform set, which is a function of Φ, the PSD objective function is also a function of phase vector Φ. It is easy to evaluate (6) in a discrete form through Fast Fourier Transform (FFT). By minimizing the PSD objective function, the candidate transmitting signal can be selected such that it meets the PSD requirement.

2.2.2. Objective Function for CCF and ACF

The objective function for CCF and ACF is built based on the total sidelobe energy of all autocorrelations plus the total energy of crosscorrelations from different waveform pairs. Mathematically, we express it as:

$$obj_{CF} = \sum_{n=1}^{N} \sum_{k=n_1}^{M-1} |ACF(\mathbf{x}_n, k)|^2 + \lambda_1 \sum_{p=1}^{N-1} \sum_{q=p+1}^{N} \sum_{k=-M+1}^{M-1} |CCF(\mathbf{x}_p, \mathbf{x}_q, k)|^2 \tag{7}$$

where n_1 defines the mainlobe width, and λ_1 is the weight balancing these two items on the right hand of (7). n_1 and λ_1 can be determined based on application requirement.

2.2.3. PSO Algorithm

PSO algorithm is a fast developing evolutionary algorithm. It is widely adopted in various areas with universal verification of its global searching ability [19–22]. Compared with other evolutionary algorithms, PSO less likely gets stuck in a local optimum due to its ability of random perturbation. In this paper, PSO algorithm is used to search for the optimal phase vector that can satisfy the waveform design requirements.

We use the standard PSO algorithm to optimize (5). The optimizer initially generates a group of, say L, random phase vectors as potential solutions. Each phase vector is called a particle with its cost value evaluated from the specified objective function. Each particle will keep track of its positions in the problem space and store the position with the best fitness value it has achieved so far as the population best, say, $\mathbf{P}_{best}$. The optimizer will also keep track of the particle position that has the best fitness value obtained so far by any particle in the population. This position is taken as the global best, say, $\mathbf{G}_{best}$. The population best and global best are initialized as below:

$$\mathbf{\Phi}^j \rightarrow \mathbf{P}_{best}^j \text{ and } \arg\min Obj_{Total}(\mathbf{\Phi}^j) \rightarrow \mathbf{G}_{best}, \quad j = 1, \ldots, L. \tag{8}$$

Iteration progress starts after initialization. In each iteration, particles are employed to evaluate their fitness values based on the objective function, and the fitness values are taken to update the $\mathbf{G}_{best}$ and $\mathbf{P}_{best}$. Afterwards each particle will be updated according to

$$\begin{aligned} \mathbf{V}(i+1) &= w \cdot \mathbf{V}(i) + c_1 \cdot \mathbf{U}(0,1) \odot (\mathbf{P}_{best}(i) - \mathbf{\Phi}(i)) \\ &\quad + c_2 \cdot \mathbf{U}(0,1) \odot (\mathbf{G}_{best}(i) - \mathbf{\Phi}(i)) \qquad (9) \\ \mathbf{\Phi}(i+1) &= \mathbf{\Phi}(i) + \mathbf{V}(i) \qquad (10) \end{aligned}$$

where $\Phi(i)$ is the particle position of the ith iteration, and $\Phi(i+1)$ is the particle position of the following iteration. $\mathbf{V}(i)$ is the velocity of the ith iteration and $\mathbf{V}(i+1)$ the next iteration. w is inertia weight. c_1 and c_2 are learning factors, and $\mathbf{U}(0,1)$ is a random vector with elements uniformly distributed in the region of $[0,1]$. Operator $\odot$ means the Hadamard matrix operator. The selection of parameters w, c_1, and c_2 can be referred to [22] and [23], that is, $c_1 = c_2 = 2$, and w has an initial value around 1 and gradually declines towards 0. PSO will iterate until the desired fitness value is achieved or a given maximum number of iterations is reached.

PSO is efficient in computation effort and memory requirements. For this waveform optimization, the main computational load for each iteration comes from the update of particle position and velocity. This step involves only element multiplication and addition, as shown in (6) and (7). Thus, the computation effort and memory requirements are

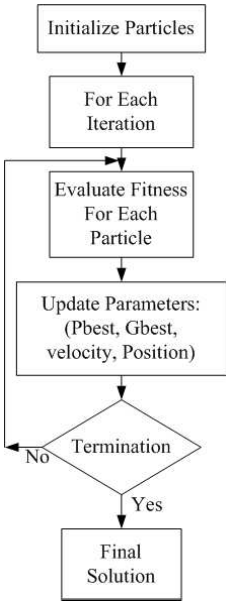

Figure 1. Flow chart of PSO algorithm.

approximately linear in the dimension of problem space *NM*. The flowchart of PSO implementation is showed in Fig. 1.

3. SIMULATION STUDY

In this section, we will evaluate the performance of the proposed method by designing several sparse frequency waveform sets. In the following case study, refereeing to (6), we set the weight $w_n(f)$ for stopband to be 10 and for passband to be 0, which means that we do not care about the shape of passband spectrum. Meanwhile, we set $P(f)$ to be 0 for stopbands and 1 for passbands.

3.1. Experiment 1: 3-stopbands

Now, let's study a relative simple case first. There are three stopbands, say, 200–220 kHz, 320–340 kHz, 400–430 kHz in total band 0–600 kHz. The sparseness, the ratio of bandwidth in all stopbands to the total bandwidth, in this case is 7/60. The pulse duration is 100 µs. We, in this case, set $n_1 = 2$, $\lambda_1 = 1$, and $\lambda = 0.5$. Fig. 2(a) shows the results of autocorrelations, Fig. 2(b) crosscorrelations, and Fig. 3 power spectral density. For the ACFs, the Peak Sidelobe

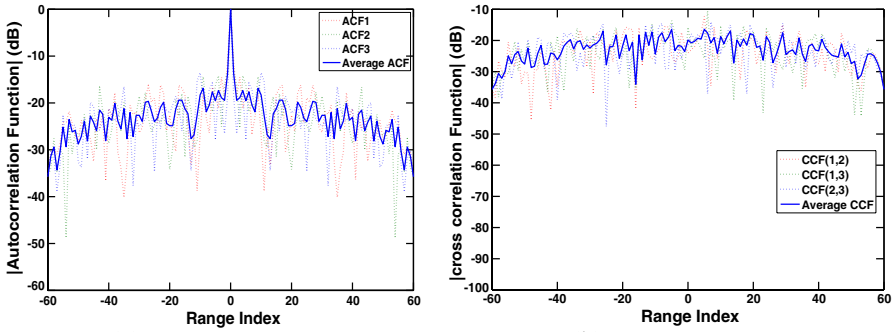

(a) ACF performance (b) CCF performance

Figure 2. Correlation performances of 3 waveforms: 3 stopbands case.

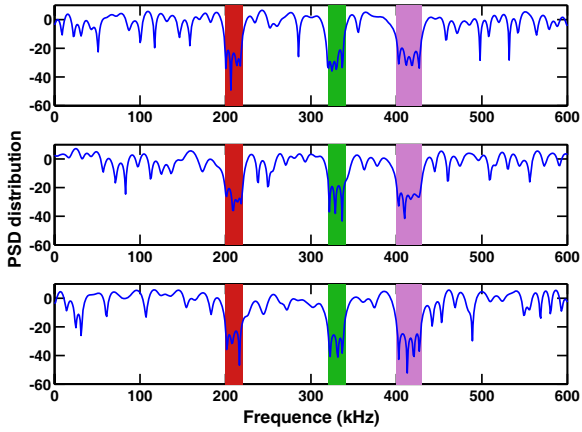

Figure 3. Power spectrum density of 3 waveforms: 3 stopbands case.

Levels (PSLs) of three waveforms are −13.5 dB, −14.2 dB, −14.6 dB, respectively. The Integrated Sidelobe Levels (ISLs) are 3.8 dB, 3.2 dB, and 3.5 dB, respectively. For the CCFs, the PSLs of three waveforms are −12.3 dB, −10.5 dB, −12.7 dB, respectively. The ISLs are 3.1 dB, 3.2 dB, and 2.9 dB, respectively. As the MIMO radar performance can, in some sense, be constrained by the ambiguity function, the averaged performance is also a metric for evaluating the set performance. We evaluate the averaged performance based on the MIMO radar ambiguity function given in [23]. The AF is given by:

$$\chi_{MIMO}(\tau, v) = \sum_{n=1}^{N} \sum_{m=1}^{N} |\chi_{nm}(\tau, v)|^2 \tag{11}$$

By setting the Doppler shift to be zero, we get the correlation function:

$$\chi_{MIMO}(\tau,0) = \sum_{n=1}^{N} |\chi_{nn}(\tau,0)|^2 + \sum_{n=1}^{N} \sum_{\substack{m=1 \\ n\neq m}}^{N} |\chi_{nm}(\tau,0)|^2$$

$$\triangleq N\chi_{ACF}(\tau,0) + \left(N^2 - N\right)\chi_{CCF}(\tau,0) \qquad (12)$$

where χ_{ACF} and χ_{CCF} are the averaged ACFs and the averaged CCFs of MIMO radar, respectively. For ACF, the averaged PSL is -16.5 dB, and the averaged ISL is 3.5 dB. For CCF, the averaged PSL is -16.9 dB, and the averaged ISL is 3.1 dB. Thus, collectively, this waveform set has better PSL performance in both ACF and CCF compared to each individual waveform. The stopband suppression in each waveform is 22.1 dB, 23.0 dB, and 25.0 dB.

3.2. Experiment 2: 5-stopbands Case

Then, let's study a relative complicated case. There are five stopbands falling in 90–160 kHz, 200–240 kHz, 320–350 kHz, 400–440 kHz, and 500–520 kHz over a total band of 0–600 kHz. The sparseness of this case is 1/3. For the parameters setting, we follow those in Section 3.1. The pulse duration is 200 µs. In this case, there are 2 times as many samples as in three-stopbands case. Fig. 4(a) shows the results of autocorrelation, Fig. 4(b) the results of crosscorrelation, and Fig. 5 the results of power spectral density. For ACF, the PSLs of three waveforms are -9.7 dB, -9.7 dB, -8.3 dB, respectively. And the averaged PSL is -9.7 dB. The ISLs are 0.35 dB, -0.11 dB, and 0.29 dB, respectively. And the averaged ISL is 0.17 dB. Compared to the results

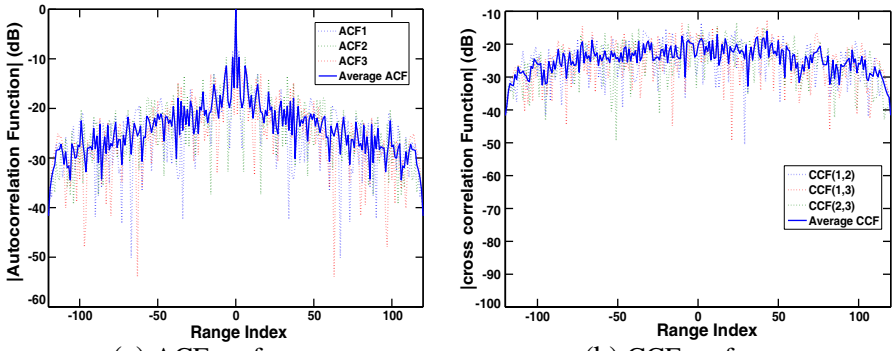

(a) ACF performance (b) CCF performance

Figure 4. Correlation performances.

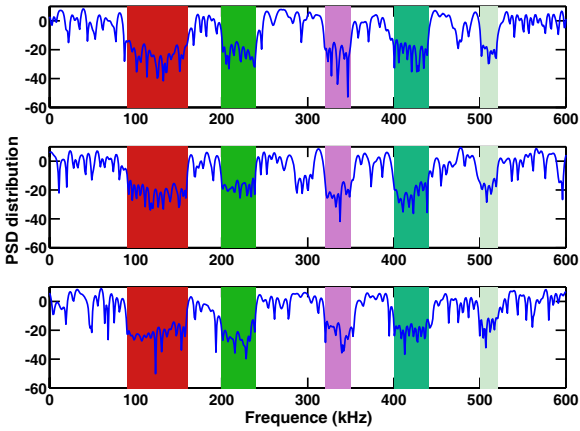

Figure 5. Power spectrum density of 3 waveforms: 5 stopbands case.

in Experiment 1, the ACF performance of each waveform in this case decreases largely. That is mainly because the sparseness of each waveform increases largely. For CCF, the PSLs of three waveforms are −14.0 dB, −13.6 dB, −13.9 dB, respectively. And the averaged PSL is −16.0 dB. The ISLs are 1.90 dB, 1.44 dB, and 1.15 dB, respectively. And the averaged ISL is 1.49 dB. Compared with Experiment 1, though the PSLs of CCFs are relatively lower in this case, the ISL performance in this case is impaired. Based on both the ACF performance and CCF performance, we can see that the sparseness has more effect on the performance of ACF than that of CCF. The stopband suppression for three waveforms is 18.3 dB, 19.8 dB, 19.2 dB, respectively.

Comparing to these two cases, we can see that due to the increase in sparseness, the total performance in case two is decreased. Meanwhile, as the PSD is an inverse Fourier transform of ACF, if we increase the suppression in stopbands, the performance in correlations will decrease, or vice versa. In addition, based on these two examples, one important point is that we can have a good chance to reduce the averaged PSL while maintaining the other performances satisfying for MIMO radar application.

3.3. Doppler Resilience

In practical operations there will be Doppler caused mismatch in the matched filter when the signal is reflected back by moving targets. Doppler effect can be illustrated by ambiguity function in general. Ambiguity function of waveform 1 in Experiment 1 is illustrated in Fig. 6, from which we can see that, as the Doppler frequency increases,

the performance degradation due to mismatch will increase. More specifically, we see the matched filter output peaks of this waveform in Fig. 7. As illustrated in Fig. 7, as long as the Doppler-time product of waveform is smaller than 0.5, the output signal amplitude will not be significantly reduced (signal loss $< 3\,\mathrm{dB}$). However, for larger Doppler-time product, the performance will degrade significantly. That is mainly because the designed waveform has random phases, and therefore it is noise-like and very sensitive to the Doppler frequency when filtered by matched filter.

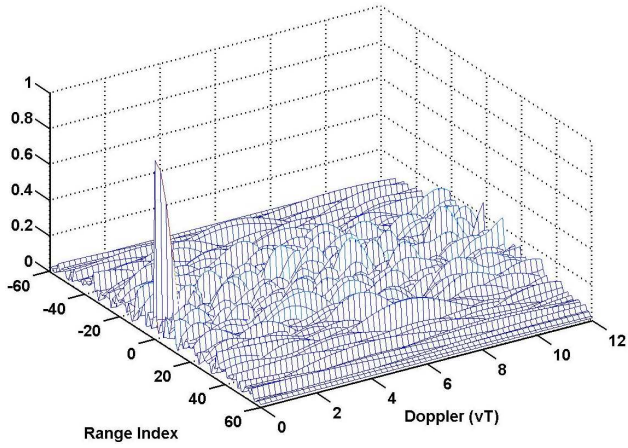

Figure 6. Ambiguity function of waveform 1 from Experiment 1.

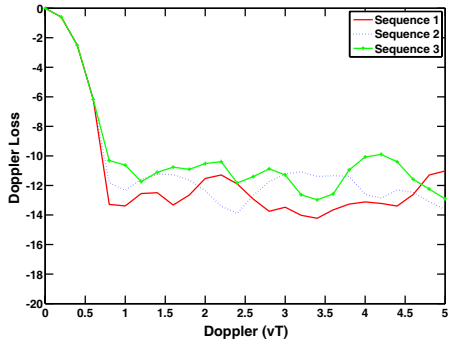

Figure 7. Matched filter output peaks of waveforms from Experiment 1.

3.4. Quantization Effects

For practical operations, the optimal phase values may be quantized before implementation in order to simplify the hardware configuration. In simulation, we can simply round down the phase values to the nearest angle bin. The loss in stopband suppression is 4.4 dB, 0.4 dB, 0.02 dB, and 0 dB for 2, 4, 8, and 16 bit quantization. Meanwhile, the PSLs of the quantized waveforms are no higher than their original counterpart. Thus, in this case, with 8-bit quantization, we can get comparable PSD and ACF performance.

4. CONCLUSIONS

In this paper, we presented a method for designing multiple sparse frequency waveforms for MIMO radar. The basic concept is to minimize a total penalty function based on both the correlation performance and power spectral density performance. Numerical examples were provided to demonstrate the effectiveness of the proposed method. A big difference compared to single waveform design is that though the individual waveform may have high PSLs in CCF and ACF, the averaged performance, i.e., the set performance evaluated by the MIMO radar ambiguity function can be far better than the individual performance. Thus, attribute to MIMO concept, we may obtain good potential to reduce the PSLs collectively rather than individually. Implementation issues such as quantization effect as well as Doppler tolerance have also been discussed.

REFERENCES

1. Fisher, E., A. Haimovich, R. Blum, L. Cimini, D. Chizhik, and R. Valenzuela, "MIMO radar: An idea whose time has come," *Proceedings of IEEE Radar Conference 2004*, 71–78, Apr. 2004.
2. Fisher, E., A. Haimovich, R. Blum, L. Cimini, D. Chizhik, and R. Valenzuela, "Spatial diversity in radars — Models and detection performance," *IEEE Transactions on Signal Processing*, Vol. 20, No. 3, 823–838, Mar. 2006.
3. Bliss, D. W. and K. W. Forsythe, "Multiple-input multiple-output (MIMO) radar and imaging: Degrees of freedom and resolution," *Proceedings of 37th Asilomar Conference on Signals, System, and Computers*, 54–59, Nov. 2003.
4. Li, J., "MIMO radar: Diversity means superiority," *Proceedings of Adaptive Sensor Array Processing-2006*, 305–309, Jun. 2006.

5. Li, J., P. Stoica, L. Xu, and W. Roberts, "On parameter identifiability of MIMO radar," *IEEE Signal Processing Letters*, Vol. 14, No. 12, 968–971, Dec. 2007.
6. Sammartino, P. F., C. J. Baker, and H. D. Griffiths, "MIMO radar performance in clutter environment," *Proceedings of 2006 CIE Radar Conference*, 1–4, Shanghai, Oct. 2006.
7. Bekkerman, I. and J. Tabrikian, "Target detection and localization using MIMO radars and sonars," *IEEE Transactions on Signal Processing*, Vol. 54, No. 10, 3873–3883, Oct. 2006.
8. Deng, H., "Polyphase code design for orthogonal netted radar systems," *IEEE Transactions on Signal Processing*, Vol. 52, No. 11, 3126–3135, Nov. 2004.
9. Khan, H. A., Y. Y. Zhang, C. Ji, C. J. Stevens, D. J. Edwards, and D. O'Brien, "Optimizing polyphase sequences for orthogonal netted radar," *IEEE Signal Processing Letters*, Vol. 13, No. 10, 589–592, Oct. 2006.
10. Li, J., P. Stoica, and X. Zhu, "MIMO radar waveform synthesis," *Proceedings of IEEE Radar Conference 2008*, 1–6, May 2008.
11. He, H., P. Stoica, and J. Li, "Designing unimodular sequence sets with good correlations — Including an application to MIMO radar," *IEEE Transactions on Signal Processing*, Vol. 57, No. 11, 4391–4405, 2009.
12. Frazer, G. J., Y. I. Abramovich, B. A. Johnson, and F. C. Robey, "Recent results in MIMO over-the-horizon radar," *Proceedings of IEEE Radar Conference*, 1–6, May 2008.
13. Lesturgie, M., "Improvement of high-frequency surface waves radar performances by use of multiple-input multiple-output configurations," *IET Radar Sonar & Navigation*, Vol. 3, 49–61, May 2008.
14. Wang, G. H. and Y. L. Lu, "High resolution MIMO-HFSWR using sparse frequency waveforms," *Proceedings of ICSP*, 1–6, Oct. 2008.
15. Lindenfeld, M. J., "Sparse frequency transmit and receive waveform design," *IEEE Trans. on Aerospace and Electronic Systems*, Vol. 40, 851–861, Jul. 2004.
16. Liu, W. X., Y. L. Lu, and M. Lesturgie, "Optimal sparse waveform design for HFSWR system," *Proc. 2007 International Waveform Diversity and Design conference*, 127–130, Pisa, Italy, May 26–30, 2007.
17. Wang, G. H. and Y. L. Lu, "Sparse frequency transmit waveform design with soft-power constraint by using PSO algorithm," *Proc. IEEE Radar 2008*, 127–130, Roma, Italy, May 2008.

18. Smith, S. T., "Optimum phase-only adaptive nulling," *IEEE Transactions on Signal Processing*, Vol. 47, No. 2, 1835–1843, Feb. 1999.
19. Kennedy, J. and R. Ebrhart, "Particle swarm optimization," *Proc. IEEE Conf. Neural Networks IV*, 1942–1948, Nov. 1995.
20. Ebrhart, R. and J. Kennedy, "A new optimizer using particle swarm theory," *Proc. Intern. Symp. Micro. Mach. Hum. Sci.*, 39–43, Apr. 1995.
21. Trelea, I. C., "The particle swarm optimization algorithm: Convergence analysis and parameter selection," *Information Processing Letters*, Vol. 85, 317–325, 2003.
22. Parsopoulos, K. E. and M. N. Vrahatis, "Recent approaches to global optimization problems through particle swarm optimization," *Natural Computing*, Vol. 1, 235–306, 2002.
23. Abramovich, Y. I., "Bounds on the volume and height distributions for the MIMO radar ambiguity function," *IEEE Signal Processing Letters*, Vol. 15, 505–508, 2008.